

# Design of a Novel Fractal Quad-Band-Notched UWB Antenna with Bionic Structure

Lei Zhang and Quanyuan Feng\*

**Abstract**—In this paper, we propose a quadruple band-notched ultra-wideband (UWB) antenna with a novel virus-mimicking structure. The proposed antenna is fed by coplanar waveguide in the FR4 material. It has a compact size of  $27 \times 29 \times 0.8 \text{ mm}^3$ . In order to reject narrowband signal interference in ultra-wideband communication, the desired notches in WiMAX (3.3–3.6 GHz), WLAN (5.1–5.8 GHz), downlink X satellite communication system (7.25–7.75 GHz), and ITU 8 GHz band (8.025–8.4 GHz) are realized. Except for these, impedance bandwidth of the designed antenna is less than  $-10 \text{ dB}$  from 2.5 GHz to 15 GHz, with average gain of 3 dBi. At the same time, it basically meets the omnidirectional requirement. With low profile and compact structure, the proposed antenna can be integrated into an ultra-wideband system, which can meet the requirements of ultra-wideband communication and improve the anti-interference ability of ultra-wideband communication.

## 1. INTRODUCTION

In 2002, the Federal Communication Commission (FCC) allowed the commercialization of 3.1–10.6 GHz band [1], then the ultra-wideband (UWB) communication technology has attracted the attention of many researchers and companies. UWB communication technology was first used in the military field, but nowadays it is widely used in cell phone mobile communication, high-speed wireless communication in vehicle internet, high-precision radar, and other fields [2, 3]. UWB communication technology has the advantages of ultra-wide bandwidth, high transmission rate, large system capacity, low power consumption, high positioning accuracy, and anti-multipath interference [4]. In recent years, it has been rapidly developed and become one of the most popular wireless communication technologies.

Since there are some pre-existing and widely used frequency bands in the range of 3.1–10.6 GHz, such as WiMAX (3.3–3.6 GHz), WLAN (5.1–5.8 GHz) and downlink X-satellite system (7.25 GHz–7.75 GHz), it leads to the interference between UWB communication and other overlapping bands, affecting the reliability of the UWB communication. Although the use of filters can filter out the overlapping signal spectrum very well, additional filters not only increase the cost of the system significantly, but also make it difficult to miniaturize and are not conducive to system integration. Therefore, many researches focus on the structure of antenna with notched-band characteristic. Adding a notched-band structure affects current distribution so as to suppress correlated frequency bands [5, 6]. Designing UWB antennas with frequency-notched characteristic is a challenging research area, and many studies [7–15] revolve around the structure of band-notch characteristic. Currently, there are several popular structures with band-notched characteristic. [7] embedded slots in the ones to achieve specific frequency notch. Some other added strips or parasitic structures near the radiating unit [8]. [9, 10] can be achieved by loading resonators or split ring resonator (SRR). Also, [11, 12] used capacitively loaded loop (CLL) resonators to achieve notched band. [13–15] used electromagnetic band gap (EBG) structures.

---

*Received 3 March 2022, Accepted 27 May 2022, Scheduled 16 June 2022*

\* Corresponding author: Quanyuan Feng (fengquanyuan@163.com).

The authors are with the School of Information Science and Technology, Southwest Jiaotong University, Chengdu 610031, China.

Using these notch structures, single or multiple notched bands can be achieved [16–29]. In [16, 17], pairs of rectangular SRR and a two via slot (TVS) EBG were respectively adopted to realize the central notched-band frequency at 6.38 GHz and 5.6 GHz. [18] attained dual-band-notched characteristics at 3.5 GHz and 5.5 GHz using a rectangular slot and a U-shaped slot. [19] implemented upper and lower WLAN dual notched bands using two L-shaped stubs external to the forked radiating patch. [20] utilized three arc-shaped slots to achieve triple notched bands. In [21], an EBG with slots was used to implement triple notches. [22] realized triple notches using a U-shaped slot and an SSR structure. [23] achieved quadruple notched bands using three U-shaped slots and one I-shaped slot. [24] implemented quadruple notched bands using a U-shaped slot and an EBG structure. [25] implemented quintuple notched bands using multiple C-shaped slots, and [26] combined U-shaped stubs and SSR to achieve sextuple notched bands. Generally, in order to achieve band-notched characteristic, the methods available in the open literature use different types of slots or stubs or adding resonant units. Most of the UWB antennas achieve single notched band, dual or triple notched bands, and a few are able to achieve more notched bands.

In this paper, we design an UWB antenna with a virus structure of quadruple notched bands, which utilizes bionics with fractal design to form a novel virus structure, covering UWB bandwidth with a compact structure and low profile. The band-notched characteristic of WLAN is achieved by digging an L-shaped slit in the ground. The U-shaped slit is etched in the feed line to achieve 8–9 GHz notch in ITU band. The SRR and V-shaped structure are embedded in the radiation patch to achieve notch bands in WiMAX and downlink X satellite communication systems, respectively. The impedance bandwidth of the antenna can cover 2.5–15 GHz while generating notches in four different frequency bands. The data from both the simulation and experimental test are used for analysis, including the reflection coefficient, gain, and radiation pattern. The results indicate that the proposed antenna performs well in the entire band and can meet the requirements for UWB communication systems. The proposed antenna is simulated and analyzed in high frequency simulation software (HFSSv18.0).

## 2. PROPOSED ANTENNA CONFIGURATION AND ANALYSIS

### 2.1. Design of Virus-Like UWB Antenna

Figure 1 illustrates the model of UWB antenna. The UWB antenna structure is designed with the help of bionics, shaped like the corona virus structure in the nature. The substrate of the proposed antenna is FR4 material with relative permittivity = 4.4 and thickness = 0.8 mm. The virus structure is realized by fractal structure iteration. Finally, the fractal antenna has  $S_{11}$  parameter below  $-10$  dB in 2.5–15 GHz, covering UWB bandwidth. The antenna is fed by coplanar waveguide and connected to an SMA connector with  $50\ \Omega$  characteristic impedance in the simulation.

The fractal antenna is based on a circular patch. The rotation transformation Equation (1) is used to form the fractal structure. The circumference of the circular patch antenna is used as the center of the iterative circle branch. Similarly, the circle branch of the first iteration is used as the basis, and

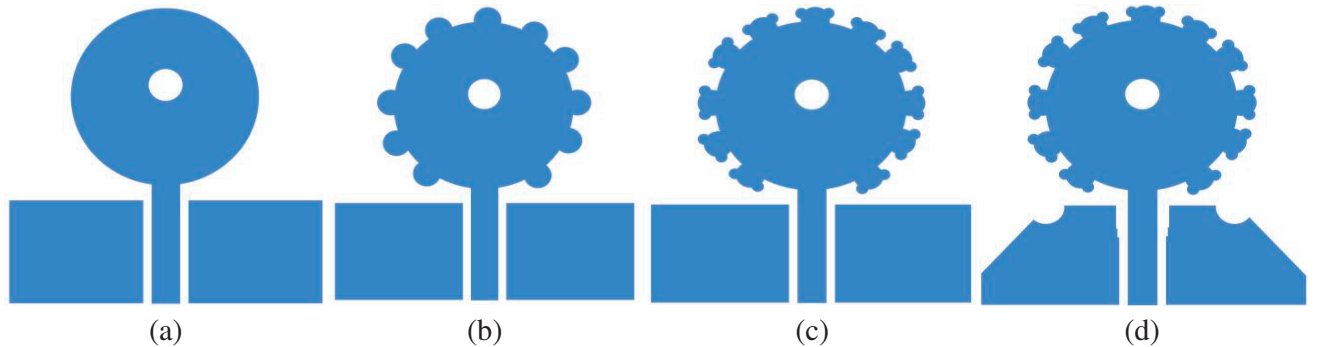


**Figure 1.** Geometry of the virus-mimicking UWB antenna. (a) Original circular structure. (b) Iteration 1. (c) Iteration 2. (d) Modified ground structure.

the next circle branch fractalizes on its circumference. After two iterations, a fractal structure similar to the virus structure is finally formed. In the two iterations, the radius of the first circle branch is 1.2 mm; the second one is 0.5 mm; and the interval degree of rotation transformation,  $\theta$ , is taken as 30 degrees.

$$\begin{bmatrix} x_n \\ y_n \end{bmatrix} = \begin{bmatrix} \cos \theta & -\sin \theta \\ \sin \theta & \cos \theta \end{bmatrix} \begin{bmatrix} R_{n-1} \\ R_{n-1} \end{bmatrix} + \begin{bmatrix} x_{n-1} \\ y_{n-1} \end{bmatrix}, \quad (1)$$

where  $(x, y)$  is the coordinate of the iterated circle in the  $X$ - $Y$  plane,  $\theta$  the rotation angle, and  $R$  the radius of the previous circle.

From Fig. 2, we can see that the bandwidth of the iterated antenna is around 2.5–15 GHz, which meets the requirement of UWB.

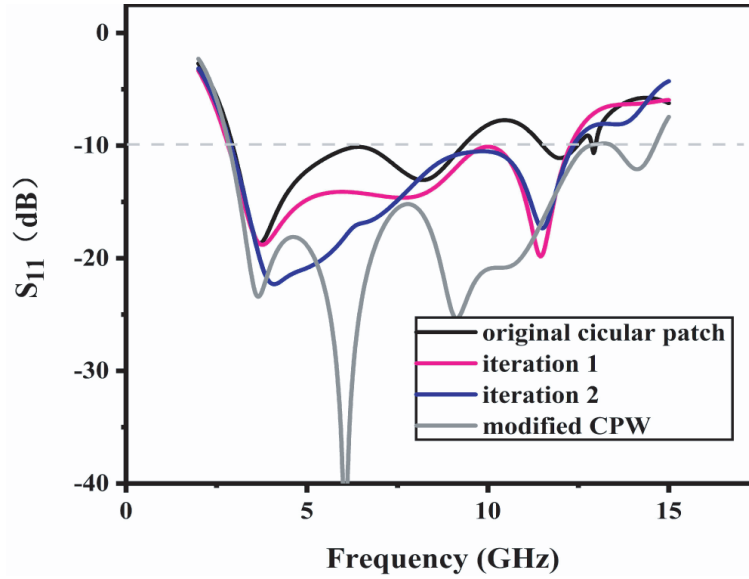


**Figure 2.** Comparison of simulated  $S_{11}$ .

Fractal antennas with normal ground basically meet the UWB requirements. For the above antenna, progressive opening is introduced in the upper side of the feed line, while conventional ground is modified into a trapezoid shape with a defected structure. The introduced progressive opening and trapezoid ground can improve impedance matching in the low band. To broaden the bandwidth and achieve better matching in the high frequency band, two circular slots are embedded in the corner of defected ground as shown in Fig. 1(d). Altering these structures appropriately improves the antenna impedance performance. Fig. 2 shows the comparison of reflection coefficient. The impedance bandwidth ranges from 2.5 GHz to 15 GHz, indicating that the bandwidth is broadened, and the curve is smoother.

## 2.2. Band-Notched UWB Antenna

Based on the designed UWB antenna above, multi-band-notched structures are introduced, with SRR structure to achieve WiMAX band notch (3.3–3.6 GHz), L-slot to achieve WLAN notch (5–6 GHz), V-slot to form notch in downlink X satellite communication band notch (7–8 GHz), and U-slot in the feed line to generate notch in ITU8 GHz band (8–8.4 GHz)

The size of the notch structure can be approximately calculated by formula (2) as follows [10]:

$$f = \frac{c}{2L\sqrt{\epsilon_{reff}}}, \quad (2)$$

$$\epsilon_{reff} = \frac{\epsilon_r + 1}{2}, \quad (3)$$

where  $L$  is the length of the notch structure,  $\varepsilon_{\text{eff}}$  the effective dielectric constant,  $\varepsilon_r$  the relative dielectric constant of the substrate, and  $c$  the speed of light in free space, taken as  $3 \times 10^8$  m/s.

The different structures of notches are shown in Fig. 3, correspondingly. Fig. 4 is the geometry of the quad-band-notched UWB antenna. The comparison of separate notch structure and quad-band-notched structure is shown in Fig. 5. From Figs. 3(a) to (d), it can be seen that every single structure is notched in the desired frequency band, 3.2–3.6, 5.0–5.8, 7.0–7.8, and 8–9 GHz, respectively, as shown in Fig. 5. Furthermore, interference excited by different adjacent structures between the notches is minimal. Hence, the notch structures are relatively independent and virtually do not affect each other.

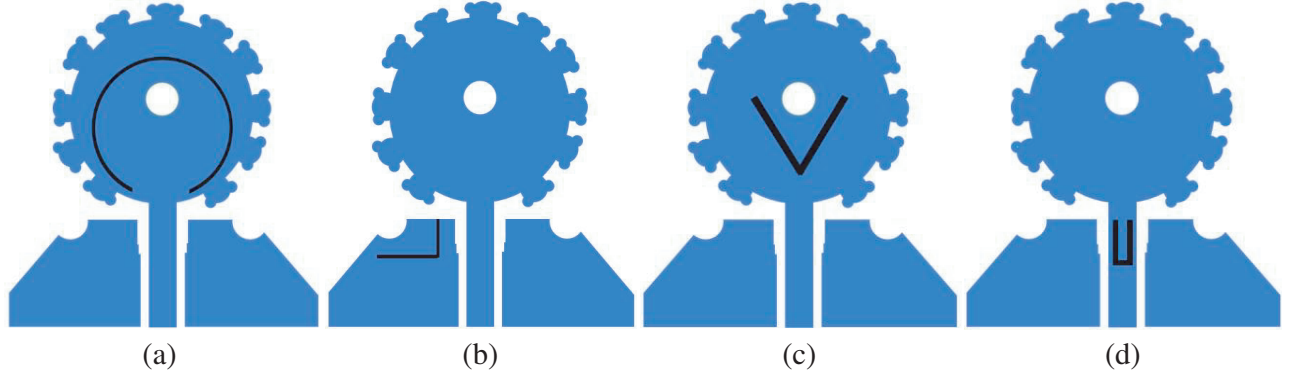


**Figure 3.** Structures of notched bands. (a)–(d) Respectively at 3.5 GHz, 5.5 GHz, 7.5 GHz and 8.2 GHz.

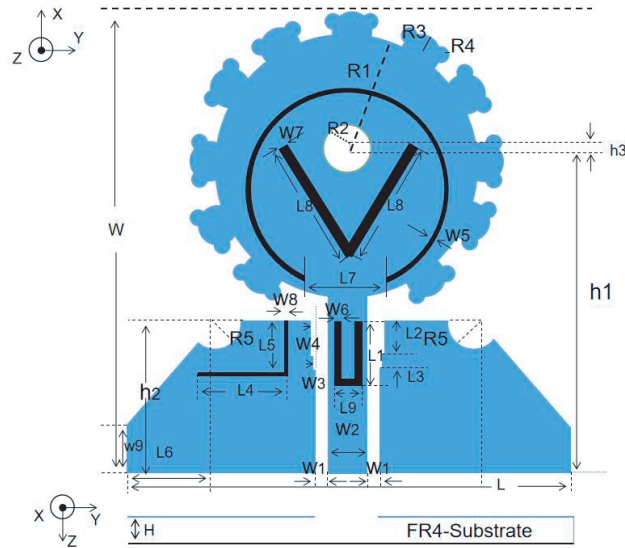


**Figure 4.** Geometry of quad-band-notched UWB antenna.

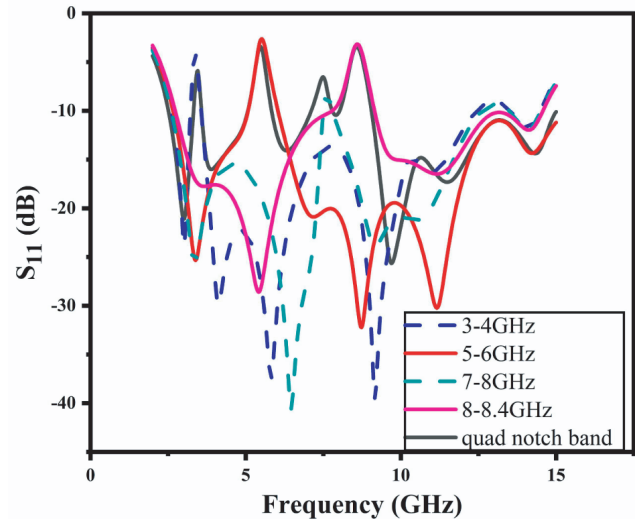


**Figure 5.** Simulated  $S_{11}$  of separate notch structure and the proposed structure.

To illustrate the band-notched mechanism, Fig. 6 shows the surface current distribution at different notched frequencies of 3.5 GHz, 5.5 GHz, 7.5 GHz, and 8.2 GHz. As shown in Fig. 6(a), the current is concentrated around the split ring at 3.5 GHz. It indicates that the split ring can suppress the radiation of this band, so as to realize the notch in WiMAX band. Similarly, the current in different frequencies is concentrated in the introduced structures, separately notched in WLAN, downlink X satellite communication system, and ITU 8 GHz band. Fig. 8 shows the real and imaginary parts of the proposed notched-band antenna. It can be seen that the real part of impedance is close to  $50 \Omega$ , and imaginary part of impedance is close to 0 in the passband, showing that it has a good impedance

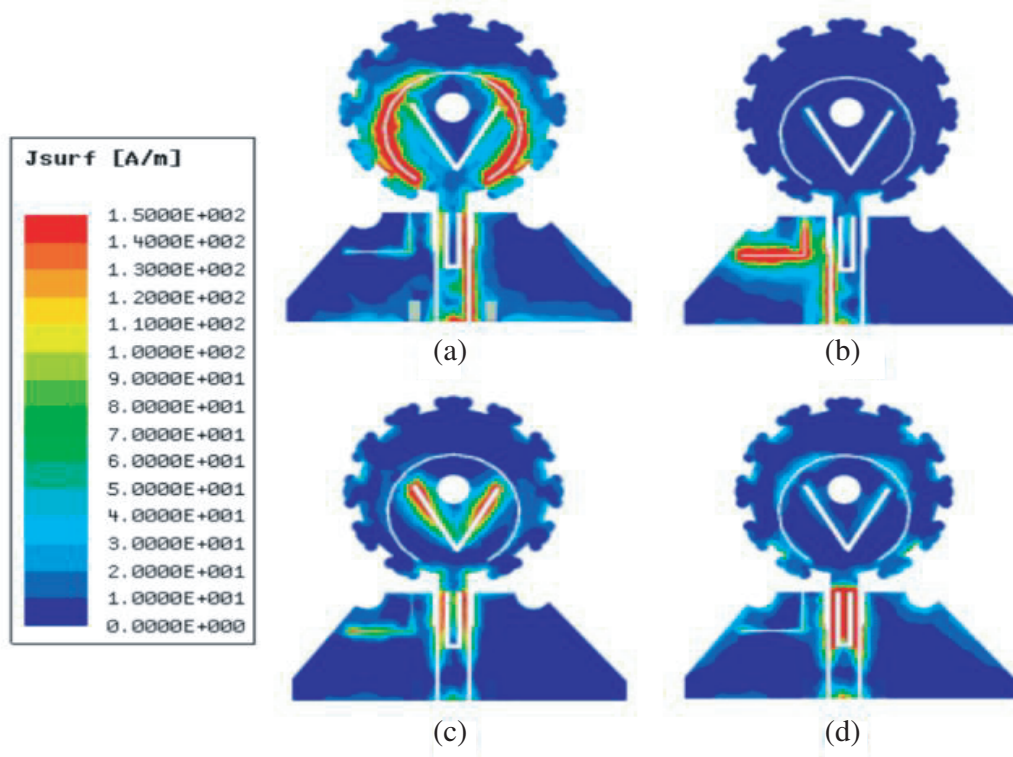


**Figure 6.** Surface current distribution in different notches. (a) 3.5 GHz. (b) 5.5 GHz. (c) 7.5 GHz. (d) 8.2 GHz.

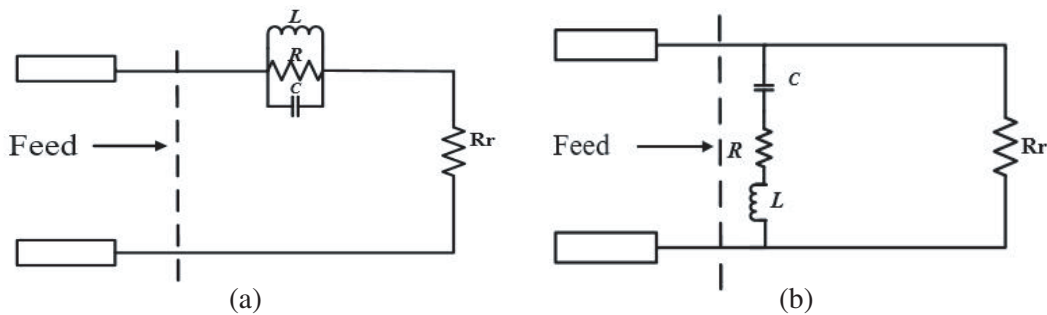


**Figure 7.** Equivalent L-C resonant circuit model for the notched-band structures. (a) At WiMAX, WLAN, and ITU8 GHz band. (b) At downlink X satellite communication band.

matching and can operate well in the passband. In the notch bands of WiMAX, WLAN, and ITU 8 GHz, real part of impedance is a high value, and imaginary part is from positive to negative value, indicating that the proposed antenna has parallel resonance characteristic in these notch bands. In the downlink X satellite communication band, the value of real part is small, and the imaginary part value is from negative to positive, showing the series resonance characteristic. The transformation of impedance matches well with the equivalent circuit model shown as Fig. 7 and can help explain the generation of corresponding the notch bands.

Equation (2) gives the approximate dimensions of the notch structure, and different lengths and widths will influence the performance of the notch. Fig. 9 shows the optimization process of the proposed antenna. By adjusting the width of the SRR structure and the length of the L-slot structure, the resonant frequency of the antenna is shifted. Fig. 9(a) shows that the width has a relatively small effect on the SRR notch structure. With the increase of  $W_5$ ,  $S_{11}$  parameter shifts slightly towards the

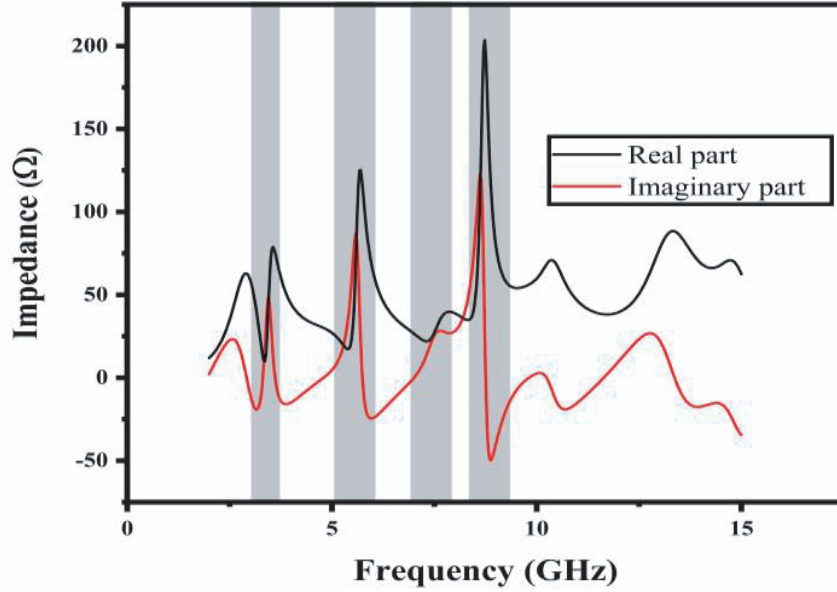


**Figure 8.** Input impedance of the proposed antenna.

left at the start frequency and the notch band in WiMAX shifts slightly to the right, showing that the impedance bandwidth remains almost constant and is not sensitive to the variations of  $W5$ . The central notch frequency is basically around 3.5 GHz, and the optimization is chosen as  $W5 = 0.3$  mm. Fig. 9(b) reveals the influence of L-slot length on notch characteristic. As the length  $L4$  increases, the center frequency drops from 6.5 GHz to 4.9 GHz with little effect on the impedance bandwidth. Correspondingly,  $L4$  is chosen as 5 mm, and the notch can cover WLAN completely. Similarly, the effect of  $L8$  and  $L1$  is shown in Figs. 9(c) and (d), and with the increase of  $L8$  and  $L1$ , the notch bands both move to the left, and the change of the notch band is regular which can help tune the notch band well. Finally,  $L8$  and  $L1$  are chosen as 7.2 mm and 5.3 mm, respectively. Table 1 shows the specific size parameters of the optimized antenna.

**Table 1.** Dimensions of the proposed antenna.

Parameters	Values (mm)	Parameters	Values (mm)	Parameters	Values (mm)
$W$	29	$L$	27	$R1$	7.7
$W1$	0.4	$L1$	5.3	$R2$	1.4
$W2$	2.2	$L2$	3	$R3$	1.2
$W3$	0.1	$L3$	0.5	$R4$	0.5
$W4$	0.15	$L4$	5	$h1$	19.5
$W5$	0.3	$L5$	3.7	$h2$	10
$W6$	0.4	$L6$	6	$h3$	0.2
$W7$	0.5	$L7$	5.5	$R5$	1.5
$W8$	0.2	$L8$	7.2	$H$	0.8
$W9$	2				

### 3. RESULT AND DISCUSSION

The fabrication of the antenna is shown in Fig. 10. The antenna is made on an FR4 dielectric substrate with dielectric constant of 4.4 and loss tangent of 0.02. The feed line is connected to an SMA connector with the impedance of  $50 \Omega$ .



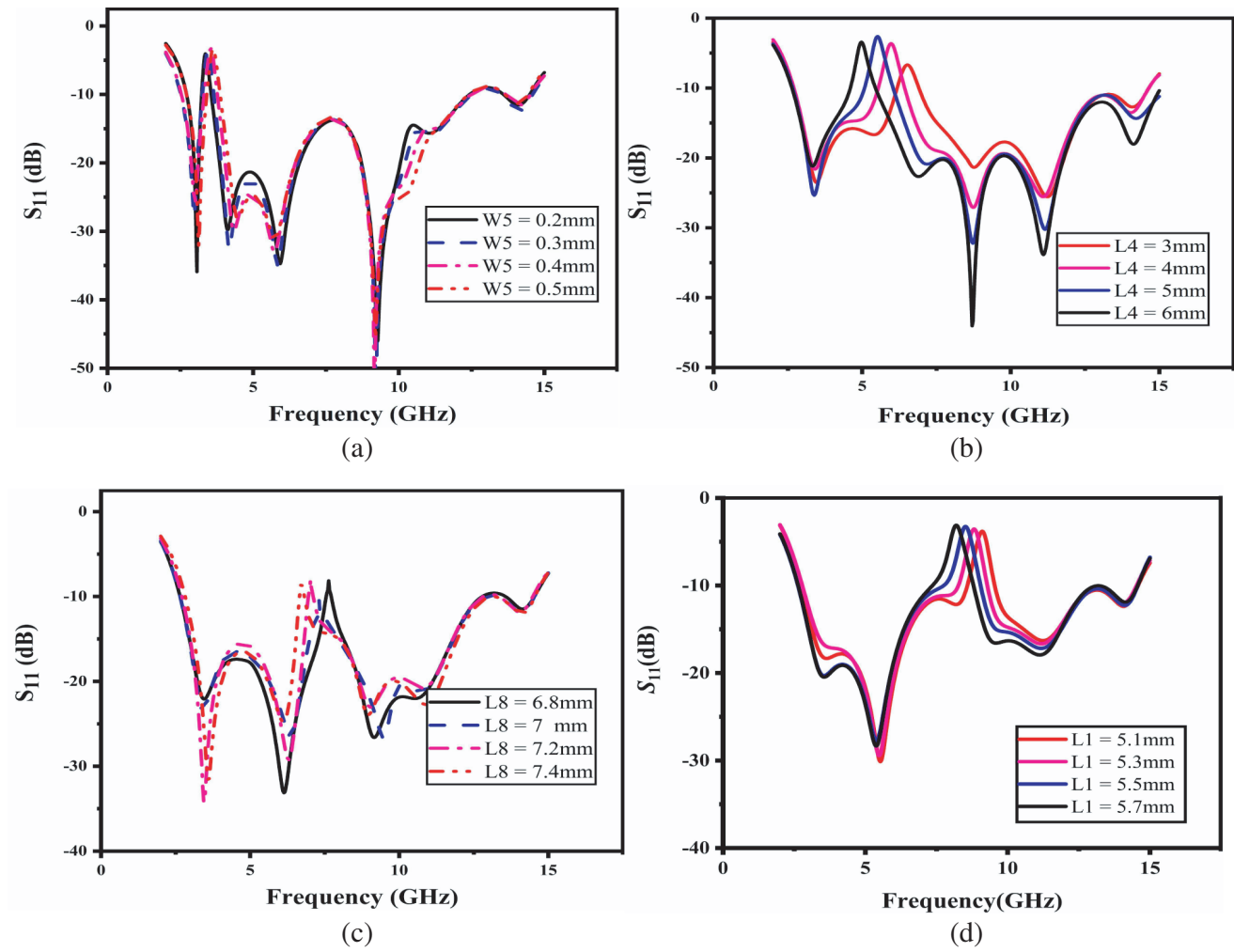


**Figure 9.** Impact of the design parameters on notch band. (a)  $W5$ . (b)  $L4$ . (c)  $L8$ . (d)  $L1$ .



**Figure 10.** Photograph of the fabricated antenna.

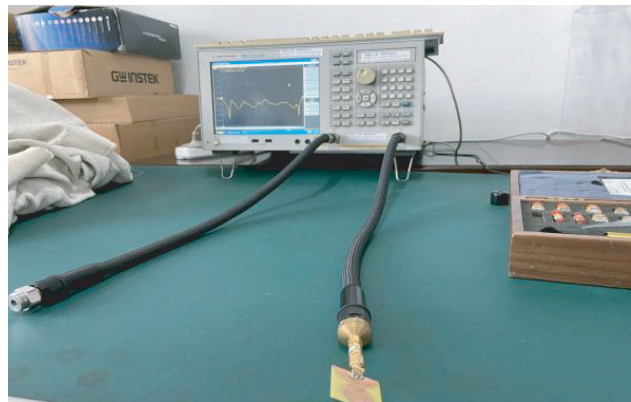


**Figure 11.** Measurement of  $S_{11}$  using VNA.

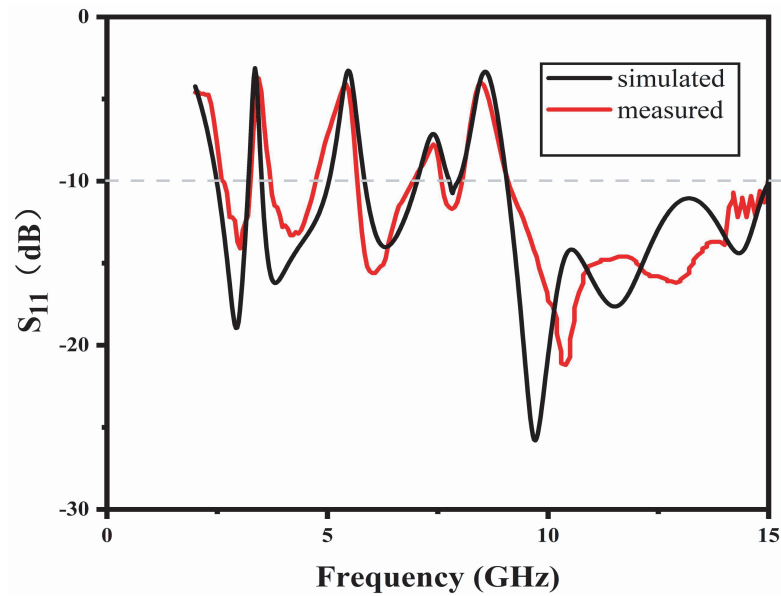


Figure 12. Comparison of  $S_{11}$  between simulated and measured.

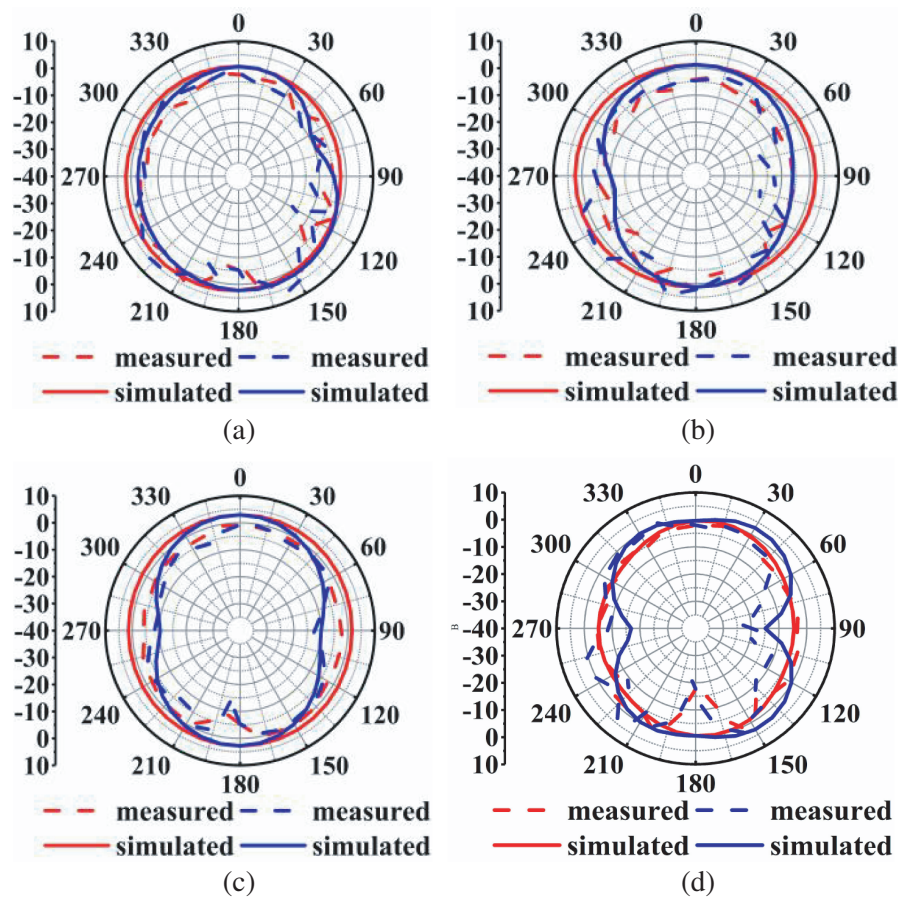


Figure 13. Simulated and measured radiation patterns. (a)–(d) Respectively at 3.1 GHz, 4.5 GHz, 6 GHz and 9.6 GHz (red represents  $X$ - $Z$  plane, blue represents  $Y$ - $Z$  plane).



In the experimental test, the  $S$ -parameter of the antenna was measured using Agilent network analyzer NE5071C as shown in Fig. 11, and the results are shown in Fig. 12. It can be seen that the antenna generates notches in the four expected frequency bands, which can reduce the related band interference. The measured result matches the simulated one relatively well. The notches in WLAN (5.1–5.8 GHz) and downlink X satellite communication system (7.25–7.75 GHz) are slightly shifted to the left. The deviation is probably due to fabrication tolerance and welding tolerance of connector. At the same time, the proposed antenna covers the entire UWB communication frequency. In addition, radiation pattern and gain are measured by a satimo anechoic chamber as shown below.

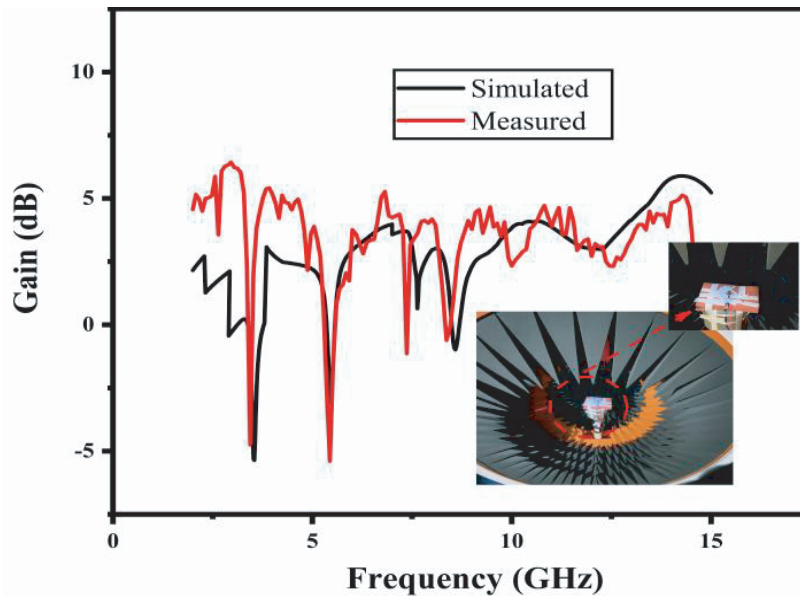


Figure 14. Measured and simulated peak gain in the anechoic chamber.

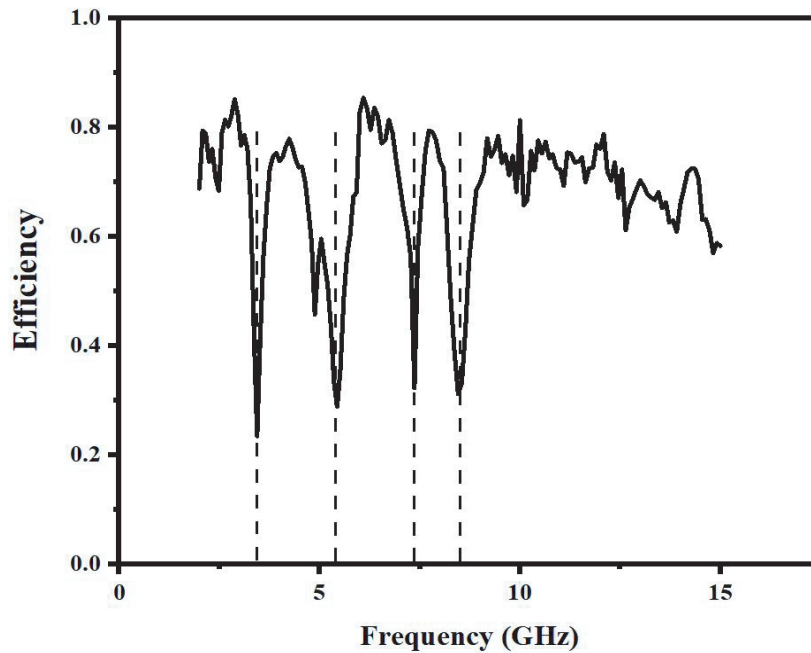


Figure 15. Measured efficiency.

Figure 13 shows the radiation patterns of the proposed antenna at frequencies of 3.1 GHz, 4.5 GHz, 6 GHz, and 9.6 GHz, indicating that the antenna has good radiation ability. In the  $X$ - $Z$  plane, the pattern shows nearly omnidirectional behavior, and the pattern shape in the  $Y$ - $Z$  plane is like a dumbbell. Despite the increase of frequency, there are some deterioration, and it still shows good radiation characteristics.

The measured and simulated peak gains are illustrated in Fig. 14. From 2.5 GHz to 15 GHz, the average of measured gain is around 3 dBi. At 3.4 GHz, 5.4 GHz, 7.4 GHz, and 8.3 GHz, the gain drops significantly to  $-4.8$  dBi,  $-5.3$  dBi,  $-1.4$  dBi, and  $-1.1$  dBi, respectively. Meanwhile, Fig. 15 shows that the measured efficiency falls rapidly in the corresponding bands. Hence, it indicates significant attenuation in these notches, and the proposed antenna can filter the interference of these bands well.

Table 2 lists the comparison between the designed antenna and the antennas in the reference papers. It can be seen that the proposed antenna is more compact and fully capable of covering the authorized UWB. The operating bandwidth ranges from 2.5 GHz to 15 GHz, having a wider bandwidth than the referenced antennas. Meanwhile, four notches are achieved in the entire band. It can be seen that good results are achieved in size of the proposed antenna and notched-band characteristic.

**Table 2.** Comparison with related antennas.

Ref.	Overall geometry (mm <sup>3</sup> )	Notch	Bandwidth (GHz)
[16]	$50 \times 50 \times 1.575$	1	3.1–10.6
[17]	$35 \times 35 \times 0.8$	1	3–12
[18]	$25 \times 38 \times 1.6$	2	2.9–15
[19]	$30 \times 30 \times 1.6$	2	2.39–2.49/3.1–11.4
[20]	$32.5 \times 30 \times 1$	3	3–12
[21]	$30 \times 31.2 \times 1.6$	3	3–12
[22]	$38.3 \times 34.5 \times 0.8$	3	2.58–11.62
[23]	$27 \times 36 \times 1.6$	4	2.8–14
[24]	$31.3 \times 34.9 \times 1.6$	4	2.9–10.5
[25]	$25 \times 31 \times 1.6$	5	3.05–10.6
[26]	$38 \times 40 \times 0.8$	6	2.85–12
[27]	$29 \times 23 \times 1.6$	2	2.91–15.3
[28]	$35 \times 25 \times 1.6$	2	2.63–13
[29]	$40 \times 38 \times 1.6$	3	2.38–13.15
Proposed	$27 \times 29 \times 0.8$	4	2.5–15

#### 4. CONCLUSION

In this paper, we design a novel fractal ultra-wideband antenna with quad-band-notched characteristic, which can cover 2.5–15 GHz, meeting the requirement of FCC authorized spectrum. The antenna adopts a bionic structure, using the self-similarity of fractal design and space-filling characteristic to form a virus-like structure. It utilizes a coplanar waveguide structure. Hence, the antenna has a compact size with low profile which can well meet the miniaturization and integration requirements, and can be integrated into the general ultra-wideband communication system. A variety of notch structures, including L-shaped, U-shaped, and V-shaped slots, and a split resonant ring, are used to achieve the notch characteristics in 3.3–3.6, 5.1–5.8, 7.1–7.8, and 8–9 GHz frequency bands. Each notch is relatively independent and does not interfere with others, which can be easily adjusted to accommodate system changes. Finally, the measured data agree well with the simulated ones, showing that the proposed antenna has stable radiation characteristics and good gain in the whole frequency band. Consequently, it can be well applied in ultra-wideband communication.

## ACKNOWLEDGMENT

This work is supported by Key Project of the National Natural Science Foundation of China under Grant 62090012, 62031016, 61831017, the Project under Grant 19-163-21-TS-001-062-01, and the Sichuan Provincial Science and Technology Important Projects under Grant 2019YFG0498, 2020YFG0282, 2020YFG0452, and 2020YFG0028.

## REFERENCES

1. Federal Communication Commission, "First report and order revision of part 15 of the Commission's rules regarding ultra-wideband transmission system," *Tech. Rep.*, ET 98-153, FCC Washington, DC, USA, 2002.
2. Ryu, K. S. and A. A. Kishk, "UWB antenna with single or dual band-notches for lower WLAN band and upper WLAN band," *IEEE Transactions on Antennas and Propagation*, Vol. 57, No. 12, 3942–3950, 2009.
3. Rahman, M. and J. D. Park, "The smallest form factor UWB antenna with quintuple rejection bands for IoT applications utilizing RSRR and RCSRR," *Sensors*, Vol. 18, No. 3, 911, 2018.
4. Chen, Z. N., "UWB antennas: From hype, promise to reality," *2007 Loughborough Antennas and Propagation Conference*, 19–22, Loughborough, UK, 2007.
5. Gao, G., B. Hu, C. Yang, and S. Wang, "Investigation of a notched UWB antenna with opening and shorting resonators," *Microwave and Optical Technology Letters*, Vol. 59, No. 7, 1733–1739, 2017.
6. Shaik, L. A., C. Saha, Y. M. M. Antar, and J. Y. Siddiqui, "An antenna advance for cognitive radio: Introducing a multilayered split ring resonator-loaded printed ultrawideband antenna with multifunctional characteristics," *IEEE Antennas and Propagation Magazine*, Vol. 60, No. 2, 20–33, 2018.
7. Ojaroudi, M., N. Ojaroudi, and N. Ghadimi, "Dual band-notched small monopole antenna with novel coupled inverted U-ring strip and novel fork-shaped slit for UWB applications," *IEEE Antennas and Wireless Propagation Letters*, Vol. 12, No. 12, 182–185, 2013.
8. Xu, H., K. Xu, W. Nie, and Y. Liu, "A coplanar waveguide fed UWB antenna using embedded E-shaped structure with WLAN band-rejection," *Frequenz*, Vol. 72, No. 7, 325–332, 2018.
9. Yadav, A., S. Agrawal, and R. P. Yadav, "SRR and S-shape slot loaded triple band notched UWB antenna," *AEU — International Journal of Electronics and Communications*, Vol. 79, 192–198, 2017.
10. Chakraborty, M., S. Pal, and N. Chattoraj, "Quad notch UWB antenna using combination of slots and split-ring resonator," *Int. J. RF Microw. Comput. Aided Eng.*, Vol. 30, No. 3, 2020.
11. Lin, C., P. Jin, and R. W. Ziolkowski, "Single, dual and tri-band-notched Ultrawideband (UWB) antennas using Capacitively Loaded Loop (CLL) resonators," *IEEE Transactions on Antennas and Propagation*, Vol. 60, No. 1, 102–109, 2012.
12. Wang, J., "Dual band-notched UWB antenna with improved radiation pattern," *Progress In Electromagnetics Research C*, Vol. 103, 59–70, 2020.
13. Peng, L. and C. Ruan, "UWB band-notched monopole antenna design using electromagnetic-bandgap structures," *IEEE Transactions on Microwave Theory and Techniques*, Vol. 59, No. 4, 1074–1081, 2011.
14. Li, T., H. Q. Zhai, G. H. Li, and C. H. Liang, "Design of compact UWB band-notched antenna by means of electromagnetic-bandgap structures," *Electronics Letters*, Vol. 48, No. 11, 608–609, 2012.
15. Ghosh, A., G. Sen, M. Kumar, and S. Das, "Design of UWB antenna integrated with dual GSM functionalities and dual notches in the UWB region using single branched EBG inspired structure," *IET Microwave Antennas Propagation*, Vol. 13, No. 10, 1564–1571, 2019.
16. Siddiqui, J. Y., C. Saha, and Y. M. M. Antar, "Compact SRR loaded UWB circular monopole antenna with frequency notch characteristics," *IEEE Transactions on Antennas and Propagation*, Vol. 62, No. 8, 4015–4020, 2014.

17. Dalal, P. and S. K. Dhull, "Upper WLAN band notch UWB monopole antenna using compact two via slot electromagnetic band gap structure," *Progress In Electromagnetics Research C*, Vol. 100, 161–171, 2020.
18. Naser, S. and N. Dib, "Printed UWB Pacman-shaped antenna with two frequency rejection bands," *Applied Computational Electromagnetics Society (ACES) Journal*, Vol. 32, No. 3, 186–192, 2017.
19. Yang, B. and S. Qu, "A compact integrated Bluetooth UWB dual-band notch antenna for automotive communications," *AEU — International Journal of Electronics and Communications*, Vol. 80, 104–113, 2017.
20. Irum Jafri, S., R. Saleem, and K. Khokhar, "CPW-fed UWB antenna with tri-band frequency notch functionality," *Applied Computational Electromagnetics Society (ACES) Journal*, Vol. 34, No. 9, 1274–1279, 2019.
21. Ghosh, A., T. Mandal, and S. Das, "Design and analysis of triple notch ultrawideband antenna using single slotted electromagnetic bandgap inspired structure," *Journal of Electromagnetic Waves and Applications*, Vol. 33, No. 11, 1391–1405, 2019.
22. Kundu, S. and S. K. Jana, "Leaf-shaped CPW-fed UWB antenna with triple notch bands for ground penetrating radar applications," *Microw Optical Technology Letters*, Vol. 60, No. 4, 930–936, 2018.
23. Jhanwar, H. S. D., M. M. Sharma, and J. K. Deegwal, "A printed monopole ellipzoidal UWB antenna with four band rejection characteristics," *AEU — International Journal of Electronics and Communications*, Vol. 83, 222–232, 2018.
24. Modak, S., T. Khan, and R. H. Laskar, "Loaded UWB monopole antenna for quadband-notched characteristics," *IETE Technical Review*, 1–9, 2021.
25. Islam, M. M., M. T. Islam, M. Samsuzzaman, and M. R. I. Faruque, "Five band-notched Ultrawide Band (UWB) antenna loaded with C-shaped slots," *Microwave Optical Technology Letters*, Vol. 57, No. 6, 1470–1475, 2015.
26. Luo, S., Y. Chen, D. Wang, Y. Liao, and Y. Li, "A monopole UWB antenna with sextuple band-notched based on SRRs and U-shaped parasitic strips," *AEU — International Journal of Electronics and Communications*, Vol. 120, 153206, 2020.
27. Hasan Mahfuz, M. M., M. R. Islam, M. H. Habaebi, N. Sakib, and A. K. M. Zakir Hossain, "A notched UWB microstrip patch antenna for 5G lower and FSS bands," *Microwave and Optical Technology Letters*, Vol. 64, No. 4, 796–802, 2022.
28. Alizadeh, F., C. Ghobadi, J. Nourinia, H. Abdi, and B. Mohammadi, "UWB dual-notched planar antenna by utilizing compact open meander slitted EBG structure," *AEU — International Journal of Electronics and Communications*, Vol. 136, 2021.
29. Kodali, R. R., P. Siddaiah, and M. N. G. Prasad, "Design of quad band operational UWB antenna with triple notch bands using meander line slot," *Progress In Electromagnetics Research M*, Vol. 109, 63–73, 2022.